Deterministic Wave Predictions from the WaMoS II

Tyson Hilmer
OceanWaveS GmbH
Lüneburg, Germany 21339
Email: hilmer@oceanwaves.de
Telephone: +49-4131-699-58-26

Eric Thornhill
Defence Research and Development Canada
Dartmouth, Nova Scotia B2Y3Z7
Email: Eric.Thornhill@drdc-rddc.gc.ca

***Abstract*—Wave induced motions limit the working time and safety of many offshore operations, e.g. crane lifts, LNG transfers, and helicopter landings. This paper details recent efforts to deterministically predict ocean surface waves using measurements from the WaMoS II. The WaMoS II derives full 3-dimensional sea surface elevation maps from nautical X-band radar images, yielding both sufficient resolution and range for a useful prediction horizon. Validation of these surface elevation fields shows they are in close agreement with sea surface elevation time series from wave buoys and motion reference units. Results from a simple propagation model are presented.**

I. Introduction

This paper evaluates the feasibility of the Wave and Surface Current Monitoring System *WaMoS II* as input to a wave prediction system. The utility of wave prediction is primarily vessel motion prediction. Specific applications include helicopter landings, liquid nitrogen gas transfers, maritime construction, small craft recovery, and crane operations. These activities are limited in their operation time due to wave induced motions which damage equipment and endanger personnel.

The task of vessel motion prediction is usually broken up into three consecutive components; 1) the derivation of ocean wave information from radar data, 2) the propagation of said ocean waves through both space and time, and 3) the vessel motion response. This paper will focus on topics (1) and (2), as these are the components limiting successful prediction.

The envisioned prediction system may provide graphical output in the form of a decision support system (Fig. 1). Predictions are updated in real-time, and evolve as new information is acquired. A colocated reference sensor, e.g. motion reference unit, provides feedback control on the prediction skill. Depending on the application, various criteria are reduced to a logical advisory whether operations may be conducted. For example, if the positive sea surface velocity exceeds the crane lift rate.

Rather than a comparison of statistical parameters, we have chosen to compare time series of sea surface elevation (SSE) between WaMoS, a Triaxys^{TM} buoy, and a XSens motion reference unit. Two key comparisons are made; colocated within the observation domain (section III), and predictions outside the observation domain (section IV). See [1] for a comparison of sea-state parameters between WaMoS and a wave measurement buoy. Prediction is not possible without sufficiently accurate input. As such, this paper focuses on the quality and accuracy of WaMoS as input to a deterministic wave prediction system. In the context of this paper, the term determinism will refer to the science of ocean surface prediction. Specifically, for a short-term (30-190 s) prediction horizon with O(cm) and sub-second accuracy and precision. Correlations values stated in this paper are coefficients of determination, commonly denoted R^2, and are calculated as the square of the sample correlation coefficient.

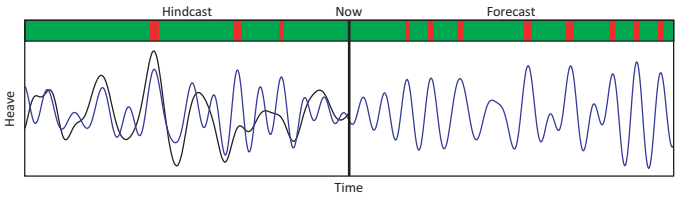

Fig. 1. Conceptual diagram of a wave prediction system. The WaMoS provides sea surface elevation estimates to a wave propagation and vessel hydrodynamic model [blue]. A motion reference unit [black] provides feedback on the prediction skill. Various criteria are tested against the prediction to yield decision support [green/red bar]. The prediction display updates in real-time.

For the prediction analysis in section IV, an overly simplified wave propagation method is employed. See [2], [3] for an analysis of the suitability of this approach for surface wave prediction. A variety of advanced wave propagation models exist including smoothed particle hydrodynamics, lattice Boltzmann, and others [4]. A short comment on computational limitations and the number of spectral coefficients with respect to wave models is given in section V.

A. Statistical vs Direct Comparison

Deterministic systems use information of the ocean state at specific locations in space and time, combined with physical laws, to predict the future ocean state. This requirement for explicit or direct measurements contrasts to the more common statistical parameter comparison. To clarify, the usual role of oceanographic measurements is as a reporting and advisory tool used to reduce the large amount of information and observed states into a few descriptive parameters. A statistical approach is the most accurate as it can utilize large sample sizes to reduce error in the parameter estimates. To understand the difficulty in obtaining accuracy in direct measurements versus statistical, a simple analogy to averaging is considered. For a measurement composed of signal and zero-mean noise, averaging of repeat measurements will improve the estimate accuracy. A single statistical parameter is often the product of thousands to millions of samples. In contrast, a single measurement will contain the full proportion of noise. Determinism requires high accuracy for each individual sample.

Along with increased measurement accuracy, determinism has the additional burden of basis accuracy. Basis refers to the frame of reference, i.e. the independent variables of space and time associated with every measurement. The bases (plural) provide an alignment for the recorded data. The bases of independent instruments invariably differ, although these differences may be insignificant for non-deterministic applications. For determinism, the bases accuracy must be at least the same order as the space-time scales of the prediction application. The characteristic time scale is a useful measure in the context, as it describes the scale over which the signal varies significantly. For ocean waves, a minimum scale of O(m) and O(s) is sufficient to capture the majority of energy.

II. WaMoS II

The WaMoS II digitizes, stores and analyzes sequences of X-band radar images to derive sea state parameters in the near range of the radar antenna (≈ 3 km). The system consists of high speed video digitizing hardware and WinWamos software installed on a standard PC. The system is capable of unattended automatic operation.

Radar measurements of the sea surface require the existence of Bragg waves corresponding to the radar wavelength. For X-band radars operating at 9.41 GHz, the Bragg waves are 1.59 cm. Capillary waves are wind-generated, and generally require a wind speed of ≈ 3 m/s for sufficient radar return. The nautical term for ocean wave signal in the radar return is "sea clutter". Longer gravity waves are visible in the sea clutter due to modulation [5]–[9] (Fig. 2). Generally, a minimum significant wave height of ≈ 0.5 m is required for the detection of surface gravity waves, with the exact limitations depending on the specific radar and installation geometry. The range at which gravity waves are detected is generally between 1-4 km, depending on the wind and wave environment as well as the radar.

A technique for deriving the 3D unambiguous ocean wave spectrum from a series of radar images was developed by Young and Rosenthal [10]. The method is based on the analysis of multiple consecutive radar images within a regular space-time domain. The data is natively helical in space-time due to the combination of a rotating antenna and 1D pulsed sampling. The Cartesian grid (Fig. 3) is typically constructed using interpolation. A Fourier transform is then applied to the Cartesian domain, with the result filtered using the wave dispersion relation (Fig. 4). See [11] for a detailed description of the WaMoS data processing method. The fundamental WaMoS output is a 3D ocean wave spectrum, from which various 2D, 1D, and scalar data products are derived. These include the significant wave height, wave period, wave direction, wave length, and surface current. Two-dimensional wave vector spectra and surface current fields are also available. The output is real-time with respect to the coherent interval of analysis which is typically ≈ 80 s.

A deterministic system requires sufficient information of the sea state in real-time. The appeal of WaMoS is its ability to measure the sea surface with high temporal and spatial resolution, combined with a large observation domain, in real-time. This contrasts with conventional oceanographic wave buoys, sonars, and pressure sensors. These instruments measure at a spatial point or small region, and do not provide information over a sufficiently large spatial domain. They are also infeasible for moving vessels.

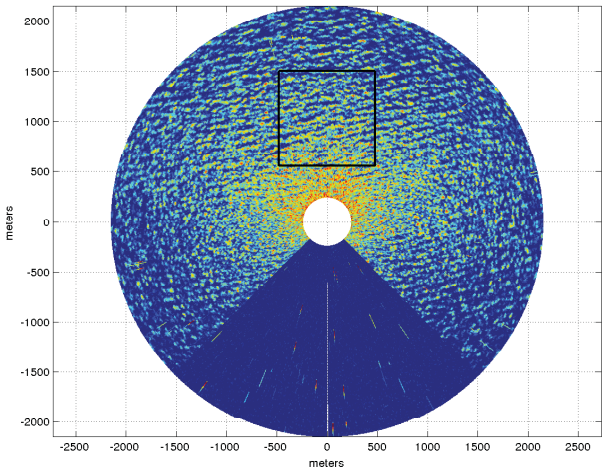

Fig. 2. An example radar image as acquired by WaMoS. Surface gravity waves are clearly visible in the raw data. An example Cartesian region [black] is used for derivation of sea state information. A "blanking sector" of data exclusion exists aft due to EM shadowing by the vessel, e.g. due to the mast or superstructure.

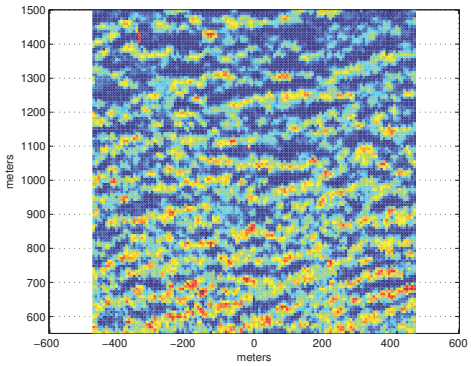

Fig. 3. An example Cartesian analysis domain used in the WaMoS processing. Only the first time sample is shown; typically either N=32 or N=64 time samples are used in the analysis. The data is natively helical in space-time and interpolated to a monotonic Cartesian domain for analysis.

For several applications, WaMoS II has proved to be a powerful tool to monitor ocean waves from coastal sites, fixed platforms, and moving vessels, especially under extreme weather conditions ([12], [13]). WaMoS II is installed worldwide at different locations. The data from these stations are mainly used to support safe navigation, off-shore or harbour operations, and weather services.

For a deterministic system, either the 3D ocean wave spectrum or 3D sea surface elevation (hereafter SSE) from the WaMoS can be used as input to the wave propagation model. These two data products are directly related via the Fourier transform.

A. WaMoS II Specifications

In the context of deterministic measurements, a discussion of the WaMoS fundamental operating parameters and the

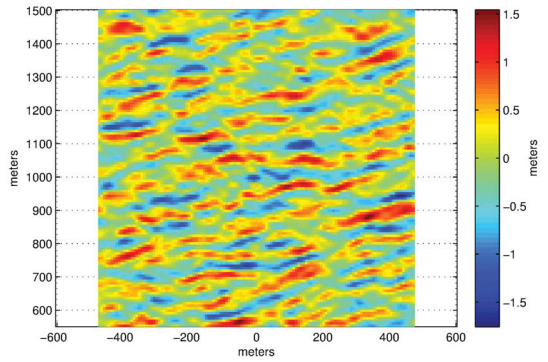

Fig. 4. An example sea surface elevation (SSE) output from WaMoS. The fundamental output of the WaMoS is a 3D ocean wave spectrum. The 3D Fourier-transform of the spectrum yields the SSE.

associated spatio-temporal resolutions is given. The aforementioned Cartesian analysis domain has arbitrary (independent) resolution and range, since interpolation is used. In practice, the Cartesian domain is chosen to correspond to the native range resolution.

The resolution in range Δr_{radar} is fundamentally limited by the pulse duration of the radar Δt_{radar} as $\Delta r_{radar} = c\Delta t_{radar}/2$ where $c \simeq 3 \times 10^8$ m/s is the velocity of light. The factor of 2 is due to the round-trip time for the electromagnetic pulse. The nominal minimal pulse duration for current commercial radars is 70 ns, while the maximum recommended pulse duration for WaMoS II is 100 ns, corresponding to Δr_{radar} in the range of 10.5-15.0 m. The WaMoS supports pulse durations down to 20 ns, i.e. 3.0 m range resolution.

The angular resolution is fundamentally limited by the radiation pattern of the radar antenna, where the antenna length is the primary factor determining angular resolution. Nominal angular resolutions, $\theta_{antenna}$, stated by radar manufacturers are within 0.75-1.5 deg. A secondary angular resolution limit is $\theta_{radar} = \Omega/F_{radar}$ where Ω is the rotation rate of the antenna and F_{radar} is the the pulse rate of the radar. Nominal rotation rates are either 0.4 or 0.8 Hz, with pulse rates commonly exceeding 2 KHz, yielding θ_{radar} angular resolutions within 0.07-0.14 deg. Thus, the data is typically oversampled by $O(10)$ with respect to the radar fundamental angular resolution. The effective tangential resolution is then $r \sin\theta_{antenna}$ where r is the range.

In summary, the WaMoS nominal range resolution of 10 m, tangential resolution[1] of 13 m, and area[2] of 1 km^2 is sufficient for deterministic measurements. Radars with high antenna rotation rates, pulse rates, transmit power, and large antenna apertures will provide increased resolution and range.

III. Buoy Comparison

To test the feasibility of WaMoS SSE as input to a deterministic system, a correlation analysis was performed against a Triaxys wave buoy. The experiment was conducted aboard the Canadian Forces Auxiliary Vessel QUEST in support of the Seakeeping Operator Guidance project, and directed by Defence Research and Development Canada. Measurements were taken in November 2012 in the North Atlantic under large wave conditions: significant wave heights within 2-6 m and peak wave periods within 8-12 s. As both the vessel and buoys were moving, bases alignment was given careful attention. The WaMoS spatial basis was calibrated using external charts and GPS measurements, yielding constant calibration offsets. The Triaxys buoys were equipped with additional GPS loggers providing increased temporal resolution (1 Hz). The WaMoS Cartesian analysis regions were centered on the expected location of the buoy, calculated as the relative difference between GPS coordinates. As the vessel was continuously moving, this reduced the data availability to times when the buoy was within the observation range of the WaMoS, nominally 2 km. A total of N=527 independent analyses were performed.

The correlation analysis was performed at a temporal rate of 6.7 Hz, corresponding to the native rate of the buoy. As the WaMoS native rate was 0.4 Hz, interpolation was required to match the time basis. It was found that Fourier series interpolation yielded greater correlations than linear interpolation (Fig. 6). Similar to linear interpolation, Fourier series interpolation does not modify the original data values at the original basis. The interpolated regions are smoothly connected via the original data values. This avoids the gradient inversions that occur from linear interpolation. WaMoS to buoy cross-correlations were calculated for a fixed coherent interval of 80 s. Together with the 0.15 s resolution, this was deemed sufficient to capture the majority of ocean wave variance.

Despite the WaMoS spatial calibration, the bases were not exactly colocated, as evidenced by varying phase shifts between the buoy and WaMoS time series (Fig. 5). Consequently, it was deemed necessary to perform a spatial-temporal search for maximum correlation. The resulting maxima in cross-correlation are an empirical estimate of the residual bases offsets. Relevant to the method of a spatial-temporal correlation search are the characteristic space and time scales of the ocean waves. For example, a monochromatic sinusoid will auto-correlate at its time scale. Searching for such a sinusoid amongst replicas (or measurements) of itself, phase shifted in space-time, is redundant past the characteristic space and time scales. For ocean surfaces described by a summation of sinusoids, autocorrelation may be used to estimate the characteristic scales. For this analysis, the time scale was taken as the time lag corresponding to the first maximum of the normalized autocorrelation function for the buoy. This value was $R_1^2 \simeq 0.6$ at a temporal lag of 3.8 s. Thus the correlation search was limited to a ± 5 s window. The normalized correlation coefficient R_1^2 of the first peak was used as a criterion for significant correlation as well as successful bases alignment, since lesser or similar magnitude cross-correlation values will occur for any arbitrary offset.

The spatial maps of cross-correlation exhibited spatial periodicity at length scales significantly greater than the peak ocean wavelength (Fig. 7). Generally, correlation maxima were within time offsets $\Delta t < 2.5$ s and spatial offsets $\Delta s < 50$ m. The spatial offsets exhibited a broad distribution throughout the entire Cartesian domain (Fig. 8). This indicated failure of the correlation search method, i.e. that the maxima did not correspond to the bases offset. A dense subset of the spatial offsets were within 50 m of the expected buoy location:

[1]For the typical Cartesian range limits of [500,1000] m

[2]For the typical Cartesian area. The total observation area is ≈ 10 km^2

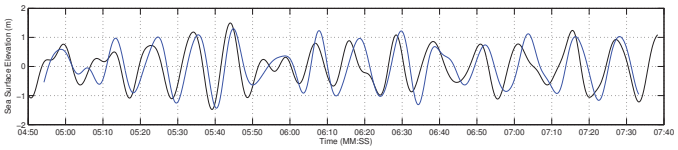

Fig. 5. Example time series comparison between the WaMoS [blue] and buoy [black]. A 1D transect is taken from the 3D WaMoS SSE, corresponding to the spatial position of the buoy. The observed phase difference is caused by bases-misalignment. The cross-correlation value is 0.56.

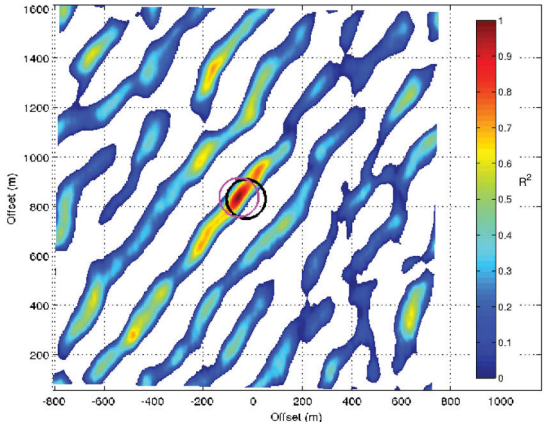

Fig. 7. Temporal cross-correlation as a function of spatial offset between the WaMoS and buoy. Only positive correlations are shown. The peak correlation $R^2 = 0.94$ [pink] was found near the expected location of the buoy [black] at a bases offset of $ds = 29.6\,\text{m}, dt = -2.91\,\text{s}$. The non-colocated correlations generally do not exceed the buoy autocorrelation $R_1^2 = 0.6$. Peak wavelength at this time was 61 m.

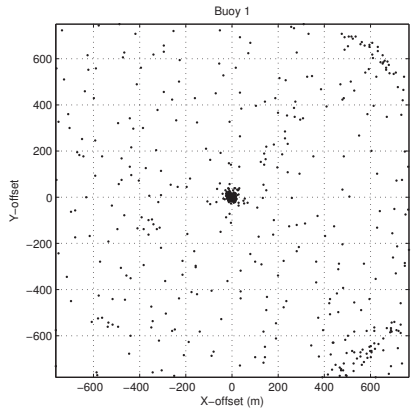

Fig. 8. Spatial offsets for correlation maximum between WaMoS and buoy. 27% of the N=527 independent analysis are within 50 m of the expected buoy location at the origin.

27% of the analyses. The correlation values for this subset had a higher mean than the total mean, $\overline{R^2} = 0.80$ and 0.72 respectively, and exceeded the significance criterion of $R^2 > R_1^2 = 0.60$ (Fig. 9) indicative of successful bases alignment. Temporal offsets for this subset were normally distributed with a mean of $\overline{\Delta s} = -0.68\,\text{s}$. Temporal offsets for all analyses were randomly distributed, again indicating failure of the search method. Time series comparisons of the bases-aligned results exhibited excellent phase, wavelength, and amplitude agreement (Fig. 6).

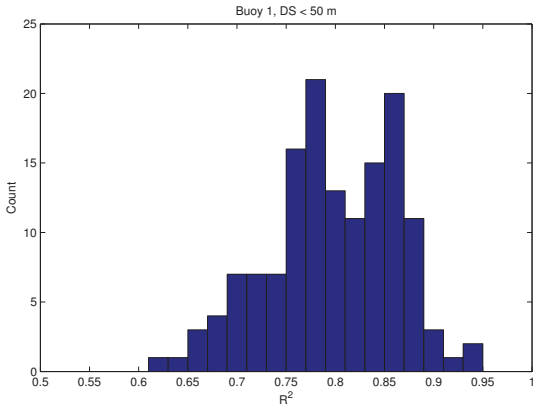

Fig. 9. Histogram of N=123 correlation values between the WaMoS and buoy. Only values corresponding to spatial offsets $\Delta s < 50\,\text{m}$ from the expected buoy location are shown. All values pass the significance test of $R^2 > R_1^2 = 0.6$

IV. Motion Reference Unit Comparison

Data for the prediction analysis was collected in the North Sea during October, 2011. Similar to section III, a cross-correlation analysis was performed between the WaMoS and an Xsens 18-degrees-of-freedom Motion Reference Unit (hereafter MRU). This analysis had the additional complication of prediction, i.e. comparison of two instruments non-colocated in space-time. The propagation model must evolve the wave information in both space and time. Spatial propagation is necessary because the radar imaging processes is fundamentally different at ranges $<\approx 300\,\text{m}$, and consequently WaMoS does not provide wave information at these ranges.

For this analysis, the WaMoS and MRU operated at 0.5 and 5 Hz, respectively. Fourier series interpolation was applied to the WaMoS SSE to match the MRU time base. The WaMoS SSE were propagated to a domain $\pm 50\,\text{m}$ following the vessel trajectory in space-time (Fig. 10), at a resolution of 5 m. This domain follows the results from the buoy colocation analysis, and the maximum expected offset of $\Delta s = 50\,\text{m}$. The domain of spatial offsets provides a Monte Carlo sampling of possible predictions.

The propagation model used was the absolute simplest method possible: phase propagation. A phase shift was applied to the WaMoS 3D spectral coefficients corresponding to the space-time translation between the measurement domain and the prediction domain. The resulting predictions exhibited broad phase variation due to the relative scale between the prediction domain and the peak wave length (Fig. 11). Averaging the predictions over the spatial domain yielded a decrease in shorter wavelengths and amplitudes, again due to deconstructive interference. The prediction following the vessel trajectory exhibited good phase agreement with the mean prediction for longer wavelengths.

The correlation search method was applied to the predictions and MRU for a 90 second coherent interval. The time offset could vary within a $\pm 30\,\text{s}$ range to allow for a time basis difference between the two instruments. For some of the analyses, the correlation maxima occurred at a prediction time of 95 s and time offset of 20 s (Fig. 12). The peak wave celerity at this time was $4.8\,\text{m/s}$. The WaMoS Cartesian domain was

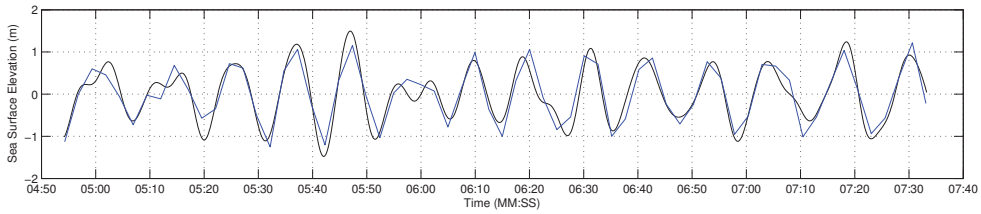

(a) Linear

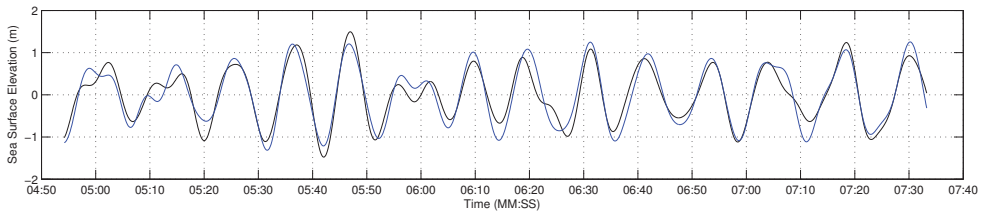

(b) Fourier Series

Fig. 6. A comparison between linear and Fourier Series interpolation methods. The WaMoS SSE time series [blue] is interpolated to match the higher frequency buoy [black]. The linear method (6a) creates gradient inversions. The Fourier Series method (6b) creates a smooth, wave-like time series. Correlation values to the buoy are 0.942 and 0.932 for the linear and Fourier Series methods, respectively. Bases alignment results in significantly greater correlation (Fig. 5).

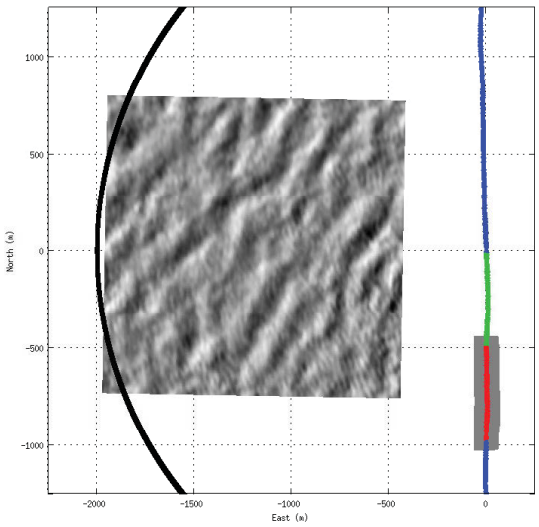

Fig. 10. Example prediction geometry. The vessel trajectory is South [blue]. WaMoS data collection [green] occurred over a time interval of 135 seconds. The Cartesian analysis region is placed in the dominant wave direction. Monte Carlo surface elevation predictions [grey] are for a future interval of 135 seconds following the vessel trajectory [red]. The nominal WaMoS observation range is 2 km [black] depending on the radar and environmental conditions.

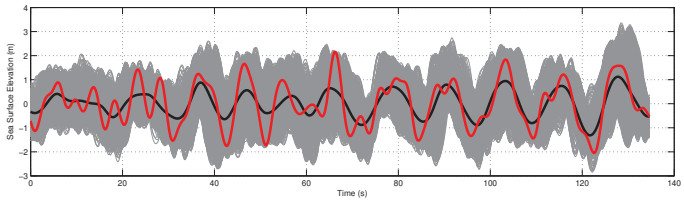

Fig. 11. Monte Carlo predictions of the sea surface elevation. The predictions [grey] are on a regular grid with 5 m resolution and +/- 50 m range about the vessel trajectory. The average prediction [black] has both reduced amplitude and loss of short wavelengths. The prediction corresponding to the vessel trajectory is indicated in red.

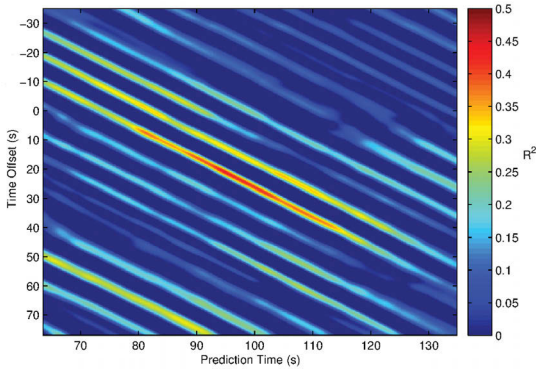

Fig. 12. Wamos and MRU cross-correlation for a 90 second coherent interval. The coherent interval begins at the prediction time of the horizontal axis. Time basis difference is evaluated as timing offsets on the vertical axis. The maximum cross-correlation occurs at a prediction time of 95 s and timing offset of 20 s.

at a distance of 500 m from the vessel, yielding a causal time difference of 104.2 s.

V. Data Reduction

Many wave models are limited in the number of input samples, either in the space or frequency domain, due to computational restrictions. Consequently, an analysis on wave coefficient reduction was performed on the WaMoS 3D spectrum.

A typical Cartesian domain has 256^2 spatial samples and 64 temporal samples for a total of $\approx 4.2 \times 10^6$ samples, and consequently an equivalent number of spectral coefficients. By the Shannon-Nyquist sampling theorem [14] this total is reduced by a factor of 2, i.e. redundant coefficients are excluded. The resulting 3D WaMoS spectrum is unambiguous in wave propagation direction (Fig. 13).

Parseval's Theorem equates the energy in a time series with the energy in the corresponding spectrum. Consequently, given a required amount of SSE variance, an equivalent amount

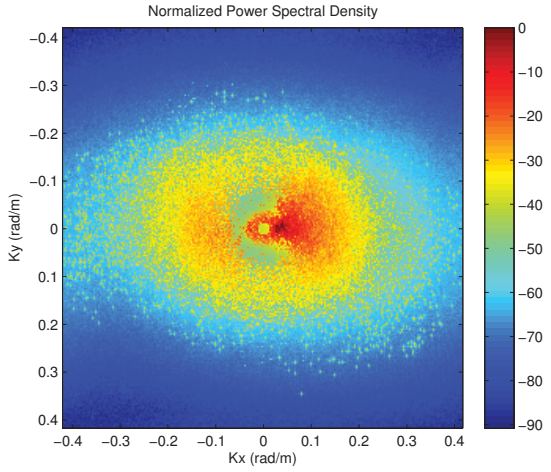

Fig. 13. Example WaMoS 2D wave vector spectrum. Integration over the positive temporal frequencies yields an unambiguous wave propagation direction, i.e. wave vector. Coefficient amplitudes are normalized power spectral density, spanning $\approx 80\,\mathrm{dB}$.

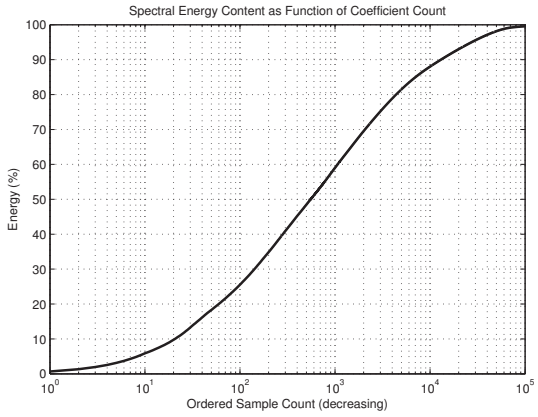

Fig. 14. Cumulative energy as a function of ordered spectral coefficient count. The total number of coefficients is $\approx 4.2 \times 10^6$ 90% of the energy is contained in the 12 500 largest coefficients, corresponding to a reduction of two orders of magnitude.

of variance can be selected from the spectral coefficients. Ordering the spectral coefficients allows the maximum amount of SSE variance to be contained in a minimum number of coefficients (Fig. 14). Using data from the aforementioned domain size of $\approx 4.2 \times 10^6$ samples, it was found that the temporal cross-correlation between the original SSE and the coefficient-reduced SSE was $\overline{R^2} = 0.90$, averaged over the spatial domain (Fig. 15h). The corresponding number of spectral coefficients and normalized spectral energy was 12,500 and 90%, respectively.

VI. Conclusion

This paper evaluates the feasibility of the Wave and Surface Current Monitoring System *WaMoS II* as input to a wave prediction system. The high spatial and temporal resolution of WaMoS, combined with the large observation area, satisfy the fundamental requirement of sufficient information for determinism.

The correlation maxima search was useful as a rough "focusing" method to achieve colocation between the WaMoS and buoy. Successful colocation resulted in high correlation values, indicating the instruments perform equivalently in resolving sea surface elevation. Presumably the WaMoS has similar performance over the full 2D spatial domain providing an ideal input for a deterministic system. Further work is required to identify the source of bases offset between the WaMoS and buoy. Comparison to an earth-fixed instrument would help characterize the WaMoS' positioning accuracy. As the spatial offsets were of similar magnitude to GPS error ($O(15)$ m), it is expected that filtering of the GPS input will be necessary to further reduce errors. Similarly, more accurate timing methods are under development for the WaMoS system.

The importance of reducing bases errors is highlighted by the estimated bases offsets. The observed values often exceed a 90 degree phase shift relative to the peak wave system. For short-term prediction systems, such offsets are the difference between useful and worthless predictions. Furthermore, bases errors must be fully characterized before the accuracy or skill of propagation models can be evaluated. The required bases accuracy loosely scales with the wave environment; predominantly long wavelength predictions are insensitive to small errors in the bases. Consequently it is recommended that future predictive efforts be conducted in large wave environments, i.e. $H_s > 3\,\mathrm{m}$ and $T_p > 10\,\mathrm{s}$.

Given unknown bases errors, Monte Carlo predictions provide a range of expected values. The usefulness of this method depends on the scale of the bases error relative to the wave environment. Relatively large bases error will result in incoherent, i.e. zero mean, predictions. Despite incoherence, such methods have utility in the expected range of values, as many decision support criteria are based on extreme values.

The MRU prediction correlation search yielded a maximum at 95 s, which was in agreement with the expected causal time difference of 104 s. Although inconclusive, this is encouraging. The time offset of 20 seconds may be due to different time bases, e.g. the current difference between the GPS and UTC time standards of GPS-UTC=16 seconds. The short 10 s duration of this correlation peak emphasizes that phase propagation is insufficient for determinism as wave dispersion requires information (measurements) to have varying prediction time offsets as a function of wavelength. This necessitates that wave estimates be assimilated into a prediction model which allows for the variable celerity of observed waves.

References

[1] P. Izquierdo, C. Soares, J. Nieto Borge, and G. Rodriguez, "A comparison of sea-state parameters from nautical radar images and buoy data," *Ocean Engineering*, 2004.

[2] P. Naiijen and E. Blondel-Couprie, "Reconstruction and prediction of short-crested seas based on the application of a 3d-fft on synthetic waves. part 1: Reconstruction," in *Proceedings of the ASME 2012 31st International Conference on Ocean, Offshore, and Arctic Engineering*, ser. OMAE2012, Rio de Janeiro, Brazil, July 2012, pp. 1–11.

[3] E. Blondel-Couprie and P. Naiijen, "Reconstruction and prediction of short-crested seas based on the application of a 3d-fft on synthetic waves. part 2: Prediction," in *Proceedings of the ASME 2012 31st International Conference on Ocean, Offshore, and Arctic Engineering*, ser. OMAE2012, Rio de Janeiro, Brazil, July 2012, pp. 1–16.

[4] W. Xiao, Y. Liu, and D. Yue, "Ocean wave prediction using large-scale phase-resolved computations," in *Proceedings of the 2009 DoD High Performance Computing Modernization Program Users Group Conference*. Washington, DC, USA: IEEE Computer Society, 2009, pp. 278–284.

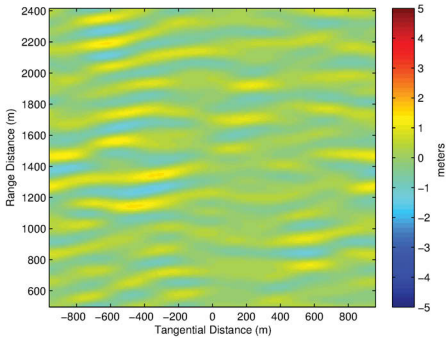

(a) N=100

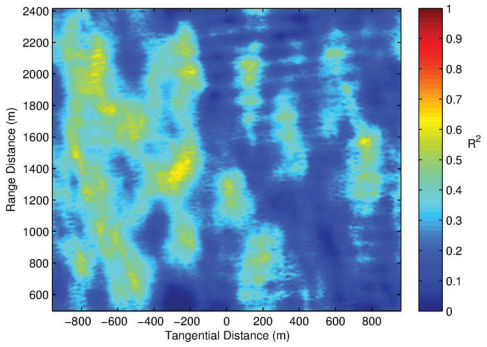

(b) N=100, $\overline{R^2} = 0.27$

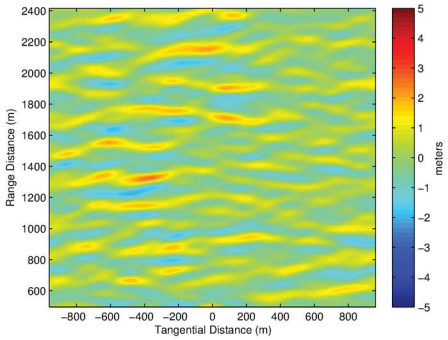

(c) N=600

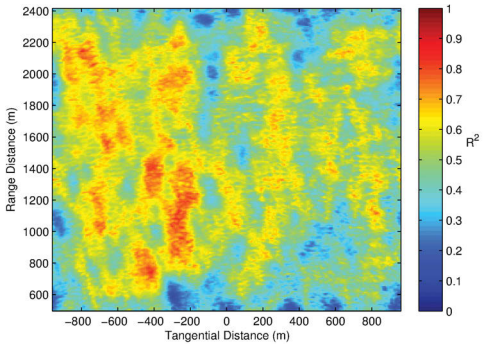

(d) N=600, $\overline{R^2} = 0.52$

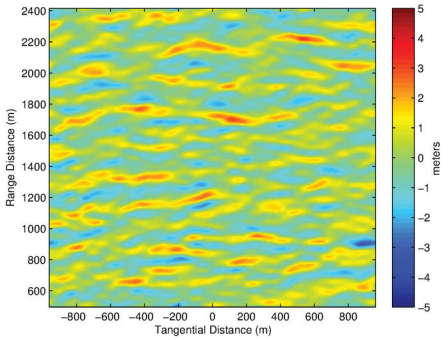

(e) N=2900

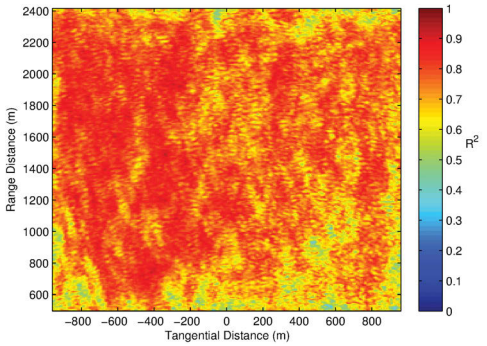

(f) N=2900, $\overline{R^2} = 0.75$

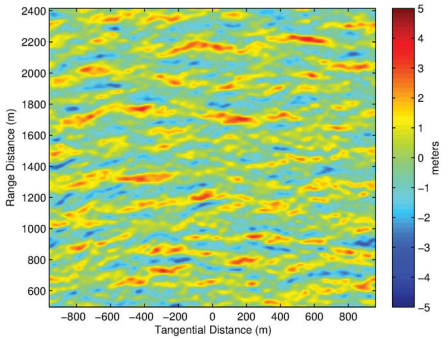

(g) N=12 500

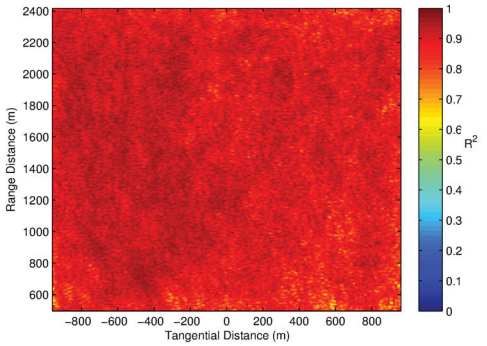

(h) N=12 500, $\overline{R^2} = 0.90$

Fig. 15. The effect of a varying number of spectral coefficients on the coefficient of determination. The temporal coefficient of determination (Figs. 15b,15d,15f,15h) between a WaMoS SSE and a coefficient-reduced SSE (Figs. 15a,15c,15e,15g) is evaluated for a varying number of coefficients. Coefficients are included in order of decreasing magnitude. 90% of the SSE variance is contained in 12 500 coefficients, whereas the original spectrum has $\approx 4.2 \times 10^6$ coefficients.

[5] W. Keller and J. Wright, "Microwave scattering and the straining of wind-generated waves," *Radio Science*, 1975.

[6] W. Alpers, D. Ross, and C. Rufenach, "On the detectability of ocean surface waves by real and synthetic aperture radar," *J. Geophys. Res.*, vol. 86, no. C7, pp. 6481–6498, 1981.

[7] W. Plant and W. Keller, "Evidence of bragg scattering in microwave doppler spectra of sea return," *J. Geophys. Res.*, 1990.

[8] L. Wetzel, *Surface Waves and Fluxes*. Netherlands: Kluwer Academic Publishers, 1990, vol. 2, ch. Electromagnetic Scattering from the Sea at Low Grazing Angles, pp. 41–108.

[9] P. Lee, J. Barter, K. Beach, C. Hindman, B. Lake, H. Rungaldier, A. Shelton, J.C. Williams, R. Yee, and H. Yuen, "X band microwave backscattering from ocean waves," *J. Geophys. Res.*, 1995.

[10] I. Young and W. Rosenthal, "A three dimensional analysis of marine radar images for the determination of ocean wave directionality and surface currents," *J. Geophys. Res.*, 1985.

[11] J. Nieto Borge, G. Rodriguez, K. Hessner, and P. Gonzalez, "Inversion of marine radar images for surface wave analysis," *Journal of Atmospheric and Oceanic Technology*, 2004.

[12] *Remote Sensing of the European Seas*. Springer Science+Business Media B.V., 2008, ch. Wave and Current Observations in European Waters by Ground-Based X-Band Radar.

[13] *Remote Sensing of the European Seas*. Springer Science+Business Media B.V., 2008, ch. Nautical Radar Measurements in Europe: Applications of WaMoS II as a Sensor for Sea State, Current, and Bathymetry.

[14] C. Shannon, "Communication in the presence of noise," *Proceedings of the Institute of Radio Engineers*, 1949.